RESEARCH ARTICLE

Morphometric and biomechanical analysis of endemic fluoride-aluminum combined poisoning

Lihua Wang[1, #], Xiuhui Zhang[2, #], Maojuan Yu[3, *]

[1]College of Public Health, Shanghai University of Medicine & Health sciences, Shanghai, China. [2]Chifeng College, Chifeng, Inner Mongolia, China. [3]College of Public Health, Guizhou Medical University, Guiyang, Guizhou, China

A rat model of coal combustion-contaminated fluorine-aluminum co-toxicity was replicated using coal-dried corn from the diseased area as the main feed along with $AlCL_3$ added to the drinking water. This study successfully established a rat model of coal-fired fluorine-aluminum co-toxicity by measuring fluorine and aluminum loading and urinary excretion and analyzing the results of dental fluorosis. Measurement and analysis of the isolated bone mineral density of the femur and tibia in rats with fluorine-aluminum co-toxicity were achieved by the application of an X-ray bone densitometer. Scanning electron microscopy was also applied to observe the morphological changes in the ultrastructure of the cancellous bone of the femur and the morphometric parameters of the bone of the upper end of the tibia of the rats during fluorine-aluminum co-toxicity. This study showed that: (1) the bone density and morphometric indicators of the high fluorine-aluminum group and high aluminum group were consistently reduced, mainly characterized by malacic skeletal fluorosis and (2) the changes in the bone tissue and morphometry in the high fluorine-aluminum group were more significant than those in the high aluminum group, suggesting a possible superimposed effect during fluorine-aluminum co-toxicity.

Keywords: fluorine-aluminum co-toxicity; bone tissue; biomechanical; bone morphometry; ultra-microstructure.

[*]**Corresponding author:** Maojuan Yu, College of Public Health, Guizhou Medical University, Guiyang, Guizhou, China. Email: 1346308505@qq.com.

[#]These authors contributed equally.

Introduction

Endemic fluorosis is a widespread disease found worldwide. In Guizhou Province, China, endemic fluorosis primarily originates from coal combustion pollution, specifically coal-burning practices employed for heating, cooking, and roasting corn and chili peppers in the affected areas [1, 2]. In 1984, a report emerged from Shuicheng County in Guizhou Province stating that the practice of roasting corn with a mixture of soil and coal had led to increased levels of fluorine and aluminum in the corn. This resulted in a local outbreak of fluorosis, characterized primarily by osteomalacia deformity [3, 4]. The use of raw coal or a mixture of raw coal and clay to dry corn in open fires caused the fluorine content of the corn to increase by several orders of magnitude, while aluminum levels increased several-fold. These substances entered the human body through the food chain and facilitated the absorption and accumulation of aluminum at certain concentrations or doses [5].

While fluoride and aluminum individually impact bone metabolism, there are divergent views on the effects of fluoride-aluminum co-toxicity on the skeletal system. Some researchers suggested

that aluminum, within a certain range, exhibited an antagonistic effect on fluoride absorption during fluoride-aluminum co-toxicity [6]. Consequently, while fluoride accumulation in the blood and bones increased with elevated fluoride intake, the addition of a specific amount of aluminum did not further augment fluoride accumulation. In an animal experiment, it was proposed that high fluoride levels facilitated the absorption and accumulation of aluminum. Therefore, controversy surrounds fluoride-aluminum co-toxicity, and research on this topic remains relatively scarce [6].

This study aimed to create a more realistic simulation of fluorosis conditions in Zhijin County, Guizhou Province, China by replicating a rat model of fluorosis using corn from the affected area. To study the combined toxicity of high levels of fluoride and aluminum, $AlCl_3$ was added to replicate a model of combined fluoride and aluminum toxicity. Changes in bone morphometry and bone tissue structure were observed using an electron microscope, providing valuable data for preventing and treating coal-burning fluorosis [7].

Materials and methods

Animal grouping and feeding methods

This study was approved by the Ethics Committee of Guizhou Medical University (Guiyang, Guizhou, China). A total of 120 Sprague-Dawley rats were obtained from the Experimental Animal Center of Guizhou Medical University two weeks after weaning. After a one-week acclimation period, the rats with the body weight (BW) of 91.1 ± 10 g were randomly divided into four groups with 30 rats per group (half male and half female). The animal room had a relative humidity of 50-60%, and the rat cage positions were adjusted weekly to ensure consistent experimental conditions. Rat growth, development, and dental changes were monitored weekly. Groups without added aluminum drank tap water containing 0.6922 mg/L (ppm) fluoride and 0.2 mg/L (ppm) aluminum. The corn consumed by the rats contained 148 mg/kg fluoride and 24 mg/kg aluminum. Based on the provisional tolerable weekly intake (PTWI) of aluminum in food (7.0 mg/kg BW) and a 100-fold safety factor between humans and animals, the high-dose group received 90 mg/L aluminum chloride, while the control group drank tap water. The high fluoride-aluminum group received 90 mg/L aluminum with 445 mg $AlCl_3$ added per liter of water. All experimental rats had free access to food and water during the exposure period. The feed formula for each group and the background fluoride and aluminum levels in the feed were listed in Table 1.

Sample collection and processing

The first batch of rats in the high fluoride group was euthanized using the femoral artery bleeding method when they showed obvious signs of dental fluorosis after 90 days of fluoride exposure. The remaining rats continued the experiment and were euthanized after 165 days of fluoride exposure using the femoral artery bleeding method. The limb bones were separated, and the muscles and connective tissues were removed. One side of the tibia was immediately placed in 4% paraformaldehyde fixative for histological sectioning and morphometric analysis. The other bones were stored at -80℃ until measurement of the bone fluoride and bone density and observations of the bone tissue using electron microscopy.

Dental fluorosis examination

The condition of dental fluorosis in the rats was examined weekly, and its occurrence and development were recorded in detail. The severity of dental fluorosis in the rats was determined, and the incidence of dental fluorosis was calculated.

Determination of fluorine load and fluorine excretion in the urine

The fluorine load in the rats was expressed as the urinary fluorine content. Urinary fluoride excretion was determined by the fluoride ion selective electrode method. Bone fluoride

Table 1. Grouping and feeding of the experimental rats.

Group	Corn from endemic fluorosis areas (%)	Corn from normal areas (%)	Other (%)	Protein* (%)	Designed value of feed fluorine (mg/kg)	Designed value of water aluminum (mg/L)	Measured value of feed fluorine (mg/kg)	Measured value of feed aluminum (mg/kg)	Measured value of feed aluminum in water (mg/L)
Control	N/A	68	32[a]	18.0	0	0	5.2	6.8	0.2
High fluorine	68	N/A	32[a]	18.0	110	0	106.0	19.7	0.2
High aluminum	N/A	68	32[a]	18.0	0	90	5.2	6.8	90.2
High fluorine-aluminum	68	N/A	32[a]	18.0	110	90	106.0	19.7	90.2

Note: a: 14.5% wheat bran, 1% bone meal and fish meal, 10% soybean flour, 5% white flour, 0.5% refined salt, and 1% yeast powder. *: 30% soybean meal, 1% bone meal and fish meal, 0.5% yeast powder and refined salt powder.

content was determined by the temperature gray-fluorine ion selective electrode method.

Aluminum in the urine and bone

With a specimen-blinded method, an inductively coupled plasma emission spectrometer (ICP) method was performed in the Guizhou Normal University Experimental Testing Center (Guiyang, Guizhou, China) to measure the aluminum in the urine and bone.

Bone density measurement

The femur and tibia from the same side of the rats were taken, and the bone density was measured using GE lunar bone densitometer (GE HealthCare Technologies, Chicago, IL, USA) and specialized software for small animals.

Tetracycline double labeling for bone histomorphometry

Ten and five days before euthanizing the rats, 1 mL of 2 mg/mL tetracycline hydrochloride solution was injected subcutaneously. The excised tibia was fixed in freshly prepared 4% paraformaldehyde for 24 hours, dehydrated in graded alcohol, embedded in non-decalcified plastic, sectioned (4 μm), stained with Goldner's trichrome stain, and analyzed using light microscopy and fluorescence microscopy. The indices included static parameters of trabecular area (mm^2), trabecular perimeter (mm), and trabecular number (per mm).

Scanning electron microscopy examination of the rat femoral trabecular bone

The femoral head (approximately 1 cm) from the same side of the rats was sagittal dissected using a surgical knife to expose the bone marrow cavity. It was rinsed with physiological saline, fixed in 4% glutaraldehyde solution for 24 hours, washed with pre-cooled phosphate buffer, soaked in osmium tetroxide for 1 hour, dehydrated in ethanol, freeze-dried in tert-butanol, directionally attached to a metal holder, sputter-coated with gold, and observed for morphological changes in the rat femoral trabecular bone ultrastructure using a Hitachi S-3400N scanning electron microscope (Hitachi, Tokyo, Japan).

Statistical analysis

The experimental data were analyzed using SPSS 26.0 statistical software (IBM, Armonk, NY, USA). Homogeneity of variances was assessed using Levene's test. Single-factor variance analysis was conducted through one-way analysis of variance (ANOVA), and post hoc multiple comparisons were performed using LSD or SNK tests when

Table 2. Changes in the average body weight (g) of the rats during the experiment.

		Days of exposure										
Group	**One week of acclimation**	**15**	**30**	**45**	**60**	**75**	**90**	**105**	**120**	**135**	**150**	**165**
Control	88.3	110.3	145.6	164.1	194.3	215.3	235.9	262.1	282.9	298.1	319.4	333.7
High fluorine	92.2	103.1	123.2	131.2	150.3	195.1	218.0	249.5	263.1	285.7	302.7	316.4
High aluminum	92.6	105.6	117.8	130.9	134.6	168.9	183.1	208.9	247.4	252.6	268.3	275.7
High fluorine-aluminum	91.2	103.2	117.3	131.7	163.4	185.1	211.1	232.6	245.9	264.2	276.8	284.5

Table 3. Fluoride levels (mg/L) in the urine of two batches of rats before euthanasia.

Group	Case	Sacrificed after 90 days of feeding	Case	Sacrificed after 165 days of feeding
Control	7	0.64 ± 0.18^{b}	6	0.69 ± 0.36^{b}
High fluorine	7	2.55 ± 0.91^{a}	5	5.50 ± 0.74^{a}
High aluminum	7	0.62 ± 0.15^{b}	6	0.67 ± 0.16^{b}
High fluorine-aluminum	7	1.86 ± 0.34^{a}	6	4.52 ± 3.09^{a}

Note: a: a comparison between each group and the control group ($P < 0.001$). b: a comparison between each group and the high fluoride-aluminum group ($P < 0.05$).

Table 4. Skeletal fluoride concentration (mg/kg) in the two batches of rats.

Group	Case	90 days	Case	165 days
Control	8	20.07 ± 3.30	9	30.06 ± 6.11
High fluorine	13	48.10 ± 13.62^{ab}	11	199.90 ± 106.84^{ab}
High aluminium	12	20.64 ± 3.02	8	25.50 ± 5.65
High fluorine-aluminium	12	59.26 ± 17.69^{a}	8	204.07 ± 63.78^{a}

Note: a: the comparison between each group and the control group ($P < 0.001$). b: the comparison between each group and the control group ($P > 0.05$)

variances were homogeneous. In cases where variances were heterogeneous, post hoc multiple comparisons were carried out using Tamhane's T2 or Dunnett's T3 tests.

Results

General condition of the rats

The rats were generally in good health with lower food intake in the experimental groups compared to the control group. In the high aluminum and high fluoride-aluminum groups, one rat in each group died, exhibiting a poor mental state, yellow fur, small stature, and eye socket bleeding. Autopsies were performed on the dead rats, and no abnormalities were found. No deaths occurred in the control or high fluoride groups. Weight gain was slower in the high aluminum and high fluoride-aluminum groups compared to the high fluoride group. Changes in the body weights of the rats in each group at different times were shown in Table 2.

Incidence of dental fluorosis

By the end of the study, no dental fluorosis was observed in either the control group or the high aluminum group. Mild dental fluorosis began to appear in the high fluoride group after about one month of fluoride exposure. In the 13th week of the experiment, severe dental fluorosis appeared in the high fluoride group. By the 24th week, the

Table 5. Urine aluminum concentration (mg/L) of the two batches of rats.

Group	Case	90 days	Case	165 days
Control	6	0.64 ± 0.20^{c}	4	0.70 ± 0.11^{c}
High aluminum	4	1.97 ± 0.56^{ab}	4	2.51 ± 0.72^{a}
High fluorine-aluminum	4	1.15 ± 0.36^{c}	4	1.48 ± 0.71^{a}

Note: a: statistical significance when compared to the control group. b: statistical significance when compared to the high fluoride-aluminum group and all other groups. c: statistical significance when compared to the high aluminum group and all other groups.

Table 6. The skeletal aluminum concentration (mg/kg) of the two batches of rats.

Group	Case	90 days	Case	165 days
Control	6	10.66 ± 3.76^{b}	5	12.66 ± 4.20^{bc}
High aluminum	6	27.07 ± 10.36^{b}	6	66.98 ± 10.37^{ab}
High fluorine-aluminum	6	214.94 ± 29.18^{ac}	4	374.21 ± 56.11^{ac}

Note: a: statistical significance when compared to the control group. b: statistical significance when compared to the high fluoride-aluminum group and all other groups. c: statistical significance when compared to the high aluminum group and all other groups.

Table 7. Measurement of rat bone mineral density (BMD).

Group	Case	90 days BMD (g/cm^2)	Case	165 days BMD (g/cm^2)
Control	4	0.1736 ± 0.0105	4	0.1854 ± 0.0198
High fluorine	4	0.1903 ± 0.0077^{b}	4	0.2053 ± 0.0107^{ab}
High aluminum	4	0.1572 ± 0.0077^{b}	4	0.1634 ± 0.0063^{ab}
High fluorine-aluminum	4	0.1389 ± 0.0058^{a}	4	0.1427 ± 0.0134^{a}

Note: a: the comparison between each group and the control group ($P < 0.05$). b: the comparison between each group and the control group ($P > 0.05$).

teeth of these rats generally showed a chalky color and deformation with severe wear visible on some rats' upper incisors.

Fluoride levels in bones and urine

Urine fluoride levels in rats exposed to fluoride were significantly higher than that in the control group ($P < 0.05$). Fluorine urine levels increased by 165 days compared to 90 days in the treated groups (Table 3). Bone fluoride levels were significantly higher in the high fluoride and high fluoride-aluminum groups compared to the control group ($P < 0.05$). Fluorine in the bones increased by 165 days compared to 90 days in the treated groups (Table 4).

Aluminum levels in urine and bone

Following a 90-day exposure to aluminum, the high aluminum group exhibited a significant increase in urinary aluminum levels compared to the control group ($P < 0.05$). After 165 days of exposure, urinary aluminum levels continued to rise compared to 90 days of exposure, and all groups exhibited a significant increase relative to the control group ($P < 0.05$) (Table 5). At the same time, all groups except the high fluoride-aluminum group showed a significant increase in bone aluminum levels compared to the control group after 90 days of exposure ($P < 0.05$). After 165 days of exposure, bone aluminum levels significantly increased compared to 90 days of exposure, and all groups exhibited a significant increase relative to the control group ($P < 0.05$) (Table 6).

Bone mineral density (BMD) measurement

After 90 days of fluorosis induction, the high fluoride-aluminum group demonstrated a statistically significant decrease in bone density compared to the control group ($P < 0.05$). After 165 days of fluorosis induction, both the high fluoride-aluminum group and the high aluminum

Table 8. Measurement of bone morphometric parameters after 90 days.

Group	Area of trabecular bone (mm^2)	Perimeter of trabecular bone (mm)	Number of trabecular bone (No./mm)	Percentage of trabecular area (%)
Control	48701.43 ± 6900.31	5902.42 ± 1017.19	25.25 ± 5.85	22.82 ± 5.83
High fluorine	62625.20 ± 1327.18*	7583.09 ± 1097.41*	41.75 ± 5.74*	18.80 ± 4.37
High aluminum	33958.45 ± 1881.44*	3661.01 ± 1317.27*	23.75 ± 12.09	15.52 ± 1.54*
High fluorine-aluminum	31667.93 ± 4234.67*	3690.09 ± 215.86*	33.00 ± 9.93	13.83 ± 3.04*

Note: *: the comparison between each experimental group and the control group ($P < 0.05$).

Table 9. Measurement of bone morphometric parameters after 165 days.

Group	Area of trabecular bone (mm^2)	Perimeter of trabecular bone (mm)	Number of trabecular bone (No./mm)	Percentage of trabecular area (%)
Control	50951.43 ± 9046.88	5672.42 ± 624.76	27.75 ± 4.19	23.82 ± 5.90
High fluorine	67612.02 ± 1662.23*	7655.44 ± 918.05*	38.25 ± 4.99*	32.70 ± 5.95*
High aluminum	38969.87 ± 1445.71	5684.10 ± 543.99	31.33 ± 14.19	32.45 ± 6.96*
High fluorine-aluminum	36073.80 ± 8851.22*	5202.20 ± 612.37	24.50 ± 2.65	16.27 ± 1.76*

Note: *: the comparison between each experimental group and the control group ($P < 0.05$).

group exhibited a statistically significant decrease in bone density compared to the control group ($P < 0.05$), while the high fluoride group showed a statistically significant increase in bone density compared to the control group ($P < 0.05$) (Table 7).

Measurement of the femoral morphometric parameters

After 90 days, the high fluoride group exhibited a statistically significant increase in the trabecular area, trabecular perimeter, trabecular number, and trabecular area percentage compared to the control group ($P < 0.05$). However, after 90 days, the high fluoride-aluminum group showed a statistically significant decrease in the trabecular area, trabecular perimeter, and trabecular area percentage compared to the control group ($P < 0.05$) (Table 8). After 165 days, the high fluoride group demonstrated a statistically significant increase in the trabecular area, trabecular perimeter, trabecular number, and trabecular area percentage compared to the control group ($P < 0.05$), while the high fluoride-aluminum group displayed a statistically significant decrease in the trabecular area and trabecular area percentage compared to the control group ($P < 0.05$) (Table 9).

Trabecular microstructure observation of rat femurs using scanning electron microscopy

Scanning electron microscopy (SEM) observations revealed that the distribution of trabeculae in the control group was uniform and well-organized, accompanied by structured collagen fibers (Figure 1a). The control group rat femur exhibited abundant trabecular bone mass. The trabeculae formed a three-dimensional network structure, extending in both the longitudinal and transverse directions. They demonstrated a moderate trabecular number, smooth surface, uniform thickness, and appropriate spacing. The collagen fibers exhibited a clear orientation, dense arrangement, and orderly organization, forming distinct bundles. The experimental groups exhibited various changes in collagen fiber morphology. The high fluoride group rat femur showed a significant increase in trabecular bone mass. The trabecular surface appeared rough and exhibited a higher degree of fusion. The collagen fibers displayed extreme disorder, with indistinct and fractured structures, resulting in a fluffy-like alteration (Figure 1b). In the high aluminum group, the collagen fibers were sparsely arranged, exhibiting a consistent orientation but varying thickness. The trabeculae displayed

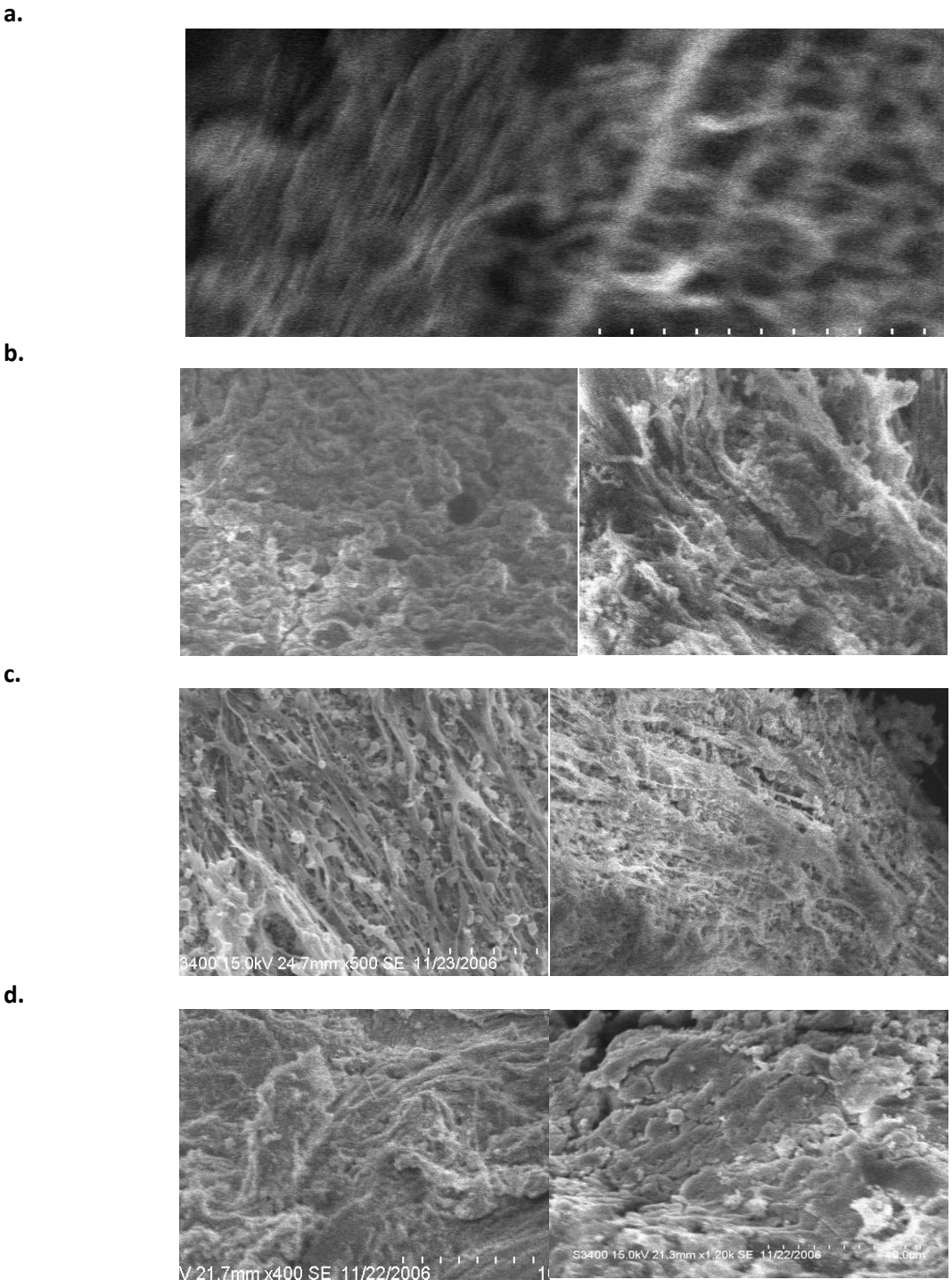

Figure 1. Collagen fibers and trabeculae in the control group (a), the high fluoride group (b), the high aluminium group (c), the high fluoride-aluminium group (d).

uneven sizes, a disordered arrangement, and notable fractures (Figure 1c). In the high fluoride and high aluminum groups, the collagen fibers appeared disorganized or plate-like, leading to the fusion of trabeculae. The surface of the trabecular bone in the high fluoride-aluminum

group was covered with a collagen-like substance characterized by thick and disordered collagen fibers. The trabeculae exhibited a random arrangement, prominent irregularities, and extensive fusion areas (Figure 1d).

Discussion

Establishment of a rat model of coal-burning type fluorosis

In this study, coal-fired corn from the fluorosis-endemic area of Guizhou Province was utilized as the primary feed. Rats were fed this diet for 165 days, and severe dental fluorosis was observed in both the high fluoride group and the high fluoride-aluminum group. The high fluoride group exhibited a significant increase in bone density compared to the control group, whereas the high fluoride-aluminum group showed a significant decrease in bone density. Based on morphometric analysis of the bone tissue, it can be concluded that the rat model of coal-burning type fluorosis was successfully replicated in this experiment [8].

The effects of fluoride-aluminum co-toxicity on bone density

During fluoride-aluminum co-toxicity, aluminum within a certain range exhibits an antagonistic effect on fluoride absorption. However, it primarily promotes fluoride absorption and enhances the toxic effect of aluminum in tissues. In this study, both the high fluoride-aluminum group and the high aluminum group demonstrated a significant reduction in bone density compared to the control group, confirming the occurrence of bone softening induced by fluoride-aluminum co-toxicity. The high fluoride group exhibited higher bone density compared to the control group, signifying the prevalence of predominantly fluorosis with hardening, consistent with the previous literature. Notably, the high fluoride-aluminum group displayed lower bone density than both the high aluminum and fluoride groups, suggesting a synergistic effect of fluoride and aluminum during exposure to high-dose fluoride-aluminum co-toxicity. Furthermore, aluminum toxicity tends to manifest as bone softening [1, 10].

The effects of fluoride-aluminum co-toxicity on rat skeletal morphometrics

Prolonged ingestion of fluoride or aluminum individually can affect the skeletal system. Chronic fluoride toxicity primarily manifests as osteosclerosis, osteoporosis, and degenerative changes in the cartilage and joints, all of which result from the disruption of the balance between bone formation and resorption, leading to a disordered arrangement of trabecular collagen fibers and a subsequent decline in the biomechanical properties of the bone [10]. The results of this study indicated that the high fluoride group predominantly experienced fluorosis with hardening, reflected by changes in the bone tissue. With prolonged fluoride exposure, these changes intensified gradually, and the morphometric parameters demonstrated an increase in bone mass, as evidenced by an augmentation of the trabecular area, trabecular perimeter, and trabecular number. Conversely, the morphometric indicators suggested a decrease in bone mass in the high fluoride-aluminum and high aluminum groups, characterized by a significant reduction in trabecular area, trabecular perimeter, and trabecular area percentage compared to the control group (the opposite of the high fluoride group). It is suggested that a softening-dominated fluorosis occurred in the high fluoride and high aluminum groups. The changes in skeletal morphometry were more pronounced in the high fluoride-aluminum group than in the high aluminum group, suggesting that under a high dose of fluoride-aluminum co-toxicity, there is an additive effect on the impact of their doses [8, 11].

Changes in bone tissue structure under electron microscopy

The trabecular bone in the high fluoride group exhibited a pronounced increase in bone mass, along with a rough and uneven surface and large fusion areas. In the high aluminum group, the

collagen fibers were sparsely arranged with inconsistent thickness, and the trabeculae varied in size, displaying a disordered arrangement and noticeable fractures. Similarly, the high fluoride-aluminum group demonstrated sparsely arranged collagen fibers with a thinner trabecular wall compared to the control group.

In this study, we investigated the bone density, osteometry parameters, and electron microscopy observations of different groups exposed to high levels of fluoride and aluminum. The findings indicate that the high fluoride group primarily exhibited sclerotic fluorosis, whereas the high aluminum group and high fluoride-aluminum group predominantly showed soft tissue fluorosis. The findings of our study suggest that in cases of co-toxicity involving high doses of fluoride and aluminum, the antagonistic effects between these elements are not significant, and there is a cumulative effect of fluoride-aluminum exposure. Furthermore, when exploring the pathogenesis and preventive measures of coal-burning fluorosis, it is crucial to consider the influence of aluminum intake [12, 13]. Additionally, among the experimental groups of rats exposed to high fluoride-aluminum and high aluminum, there were instances of mortality. However, upon dissection, no abnormalities were detected, necessitating further investigation to determine the exact cause of death while excluding potential interfering factors. Therefore, comprehensive studies on aluminum toxicity are warranted to deepen our understanding of this subject.

Conclusion

This study has successfully replicated a model of fluorine-aluminium co-toxicity in rats. In the high fluorine group, changes in bone tissue and morphometry were mainly characterized by sclerous skeletal fluorosis. In contrast, the high fluorine-aluminium and high aluminium groups exhibited changes in bone tissue and morphometry manifesting as malacic skeletal fluorosis. The changes in the high fluorine-aluminium group were more significant than those in the high aluminium group alone, suggesting a superimposed effect during fluorine-aluminium co-toxicity.

Acknowledgements

This study was supported by National Natural Science Foundation of China (Grant No. 81560511). The authors would like to thank Xiangya Medical College for the support and help in electron microscopy analysis.

References

1. Spencer H, Kramer L, Norris C, Wiatrowski E. 1981. Effect of aluminium hydroxide on plasma fluoride and fluoride excretion during a high fluoride intake in man. Toxicol Appl Pharmacol. 58(1):140-144.
2. Qin X, Wang S, Yu M, Zhang L, Li X, Zuo Z, *et al*. 2009. Child skeletal fluorosis from indoor burning of coal in southwestern China. J Environ Public Health. 2009:1-7.
3. Li FC. 1988. Report on diseases caused by coal-baked corn contaminated with kaolin. Chinese Journal of Preventive Medicine. 22(4):225-229.
4. Li FC, Liang Q, Xuzi C. 2011. Skeletal deformities in children with endemic fluorosis in Shuicheng County, Guizhou Province. Chinese Journal of Endemic Diseases. 30(2):197-201.
5. Li F. 2001. A survey of environmental factors in a sick area of coal-dried corn with aluminium-fluoride combination poisoning. Guangdong Trace Element Science. 8:37-40.
6. Wang L, Qin X, Yu M, Feng T. 2018. Exploration of changes in bone metabolism factors in coal-fired chondrodystrophic rats with fluorosis. Chinese Journal of Control of Endemic Diseases. 33:5-7.
7. Wang L, Qin X, Yu M. 2023. The influence of interventional measures on metabolic factors in fluoride and aluminium combined poisoning bones. Biotechnol Genet Eng Rev. 2:1-12.
8. Collins MT, Marcucci G, Anders HJ, Beltrami G, Cauley JA, Ebeling PR, *et al*. 2022. Skeletal and extraskeletal disorders of biomineralization. Nat Rev Endocrinol. 18(8):473-489.
9. Sun XJ, Yu YN, Xiao YM. 2010. The influence of fluoride on expression of OPGL and M-CSF genes and their proteins in rats with experimental fluorosis and the therapeutic effect of Danlan Xianpeng Liaofu capsule. Chinese Journal of Pathology. 39(10):695-700.
10. Deng CN, Yu YN, Xie Y, Zhao LN. 2013. Expression of calcineurin and nuclear factor of activated T cells 1 in testis of rats with chronic fluorosis. Chinese Journal of Preventive Medicine. 47(12):1142-1147.
11. Luo KL, Li L, Zhang SX. 2011. Coal-burning roasted corn and chili as the cause of dental fluorosis for children in southwestern China. J Hazard Mater. 185(2-3):1340-1347.
12. Xiao YH, Sun F, Li CB, Shi JQ, Gu J, Xie C, *et al*. 2011. Effect of endemic fluoride poisoning caused by coal burning on the oxidative stress in rat testis. Acta Academiae Medicinae Sinicae. 33(4):357-361.

13. Li L, Luo KL, Liu YL, Xu YX. 2012. The pollution control of fluorine and arsenic in roasted corn in "coal-burning" fluorosis area Yunnan, China. J Hazard Mater. 229-230:57-65.